Universal characteristics of particle shape evolution by bed-load chipping

GEOPHYSICS

Universal characteristics of particle shape evolution by bed-load chipping

Tímea Novák-Szabó,[1,2] András Árpád Sipos,[2,3] Sam Shaw,[1] Duccio Bertoni,[4,5] Alessandro Pozzebon,[6] Edoardo Grottoli,[5] Giovanni Sarti,[4] Paolo Ciavola,[5] Gábor Domokos,[2,3] Douglas J. Jerolmack[1,7]*

River currents, wind, and waves drive bed-load transport, in which sediment particles collide with each other and Earth's surface. A generic consequence is impact attrition and rounding of particles as a result of chipping, often referred to in geological literature as abrasion. Recent studies have shown that the rounding of river pebbles can be modeled as diffusion of surface curvature, indicating that geometric aspects of impact attrition are insensitive to details of collisions and material properties. We present data from fluvial, aeolian, and coastal environments and laboratory experiments that suggest a common relation between circularity and mass attrition for particles transported as bed load. Theory and simulations demonstrate that universal characteristics of shape evolution arise because of three constraints: (i) Initial particles are mildly elongated fragments, (ii) particles collide with similarly-sized particles or the bed, and (iii) collision energy is small enough that chipping dominates over fragmentation but large enough that sliding friction is negligible. We show that bed-load transport selects these constraints, providing the foundation to estimate a particle's attrition rate from its shape alone in most sedimentary environments. These findings may be used to determine the contribution of attrition to downstream fining in rivers and deserts and to infer transport conditions using only images of sediment grains.

INTRODUCTION

Anyone who has marveled at beach glass, admired smooth river pebbles, or examined dune sands under a microscope has an intuitive understanding that sediment transport can round particles. Centuries of field observations (*1*–*5*) and laboratory experiments (*1*, *6*–*12*) confirm that particles progressively round with increasing travel distance. Hence, particle shape has been used to infer transport environment and provenance of grains. This rounding is the result of collisions of particles with each other and Earth's surface, which acts to wear away preferentially at sharp corners and edges (*1*, *6*, *7*, *9*, *12*). It has been estimated that river pebbles, for example, may lose up to 50% of their initial mass because of gradual rounding as they are transported downstream (*5*, *7*, *12*).

In geological literature, the loss of particle mass by transport is often termed "abrasion" regardless of mechanism, whereas the meaning of abrasion is much more restricted in engineering (see below). To avoid confusion, in this paper, we refer to generic mass reduction as "attrition" (*13*, *14*). There are three relevant attrition mechanisms for sediment transport, in order of ascending energy: frictional abrasion, chipping, and fragmentation. For very low energy collisions, particle momentum is dissipated by fluid viscosity, and impact attrition cannot occur (*15*, *16*). In water, this means that particles smaller than ~10 mm in diameter experience little attrition under sediment transport. At energy levels sufficient to cause rolling and sliding of particles and to overwhelm viscous damping, frictional abrasion drives planation of faces and leads to the formation of flat or cylindrical particles (*17*). Disk-shaped pebbles observed at the margins of wave-worked beaches indicate dominance of frictional abrasion in these settings (*2*, *3*). Chipping occurs for larger energy collisions, in which impact indentation forms shallow cracks that lead to spallation production of much smaller pieces (*14*, *16*). Chipping preferentially attacks the edges and corners of the parent grain, leading to rounding and the evolution of particles toward a spherical shape (*12*, *14*). It has been shown that chipping results in a linear relation between attrition mass (δm), and collision impact energy E_i and particle size l, $\delta m \propto \alpha l E_i$, where α is a collection of material parameters that determine susceptibility to attrition (*14*). Experiments in air and water, designed to simulate bed-load transport, exhibit mass loss trends that are consistent with this relation (*10*, *18*). River pebbles moved by bed-load transport (*19*, *20*), and volcanic rocks transported in pyroclastic flows (*11*), also exhibit downstream rounding patterns that are consistent with chipping. At sufficiently large collision energies, fractures can propagate throughout a particle and lead to its breakup by fragmentation (*21*–*23*). Fatigue failure occurs when fractures grow slowly because of repeated collisions (*24*), generally causing a particle to split into a small number of pieces. Crushing results under intense loading, when explosive fracture growth leads to the disintegration of a rock into myriad smaller pieces (*21*). In all cases, fragmentation creates irregular and nonrounded particles. Remarkably, a recent study (*25*) has shown that regardless of how fragments are formed—whether by slow weathering or rapid breakup—they exhibit universal shape characteristics that are the geometric consequence of brittle fracture. Energetic gravity flows such as landslides, rock falls, debris flows, and pyroclastic flows (*11*, *26*) have been observed to produce fragmented grains, which typically serve as the source of coarse sediment for water-driven transport in rivers and coasts.

A recent study used field data and laboratory experiments to propose that the rounding of river pebbles follows a generic curve when cast as a function of the mass of material removed by chipping (*20*). Rotating drum experiments of volcanic rock fragments, meant to

[1]Department of Earth and Environmental Science, University of Pennsylvania, 240 South 33rd Street, Philadelphia, PA 19104, USA. [2]Department of Mechanics, Materials and Structures, Budapest University of Technology and Economics, Műegyetem rkp. 1-3. K261, 1111 Budapest, Hungary. [3]MTA-BME Morphodynamics Research Group, Budapest University of Technology and Economics, Műegyetem rkp. 1-3. K261, 1111 Budapest, Hungary. [4]Department of Earth Sciences, University of Pisa, Via Santa Maria 53, 56126 Pisa, Italy. [5]Department of Physics and Earth Sciences, University of Ferrara, Via Saragat 1, 44100 Ferrara, Italy. [6]Department of Information Engineering, University of Siena, Via Roma 56, 53100 Siena, Italy. [7]Department of Mechanical Engineering and Applied Mechanics, University of Pennsylvania, 220 South 33rd Street, Philadelphia, PA 19104, USA.
*Corresponding author. Email: sediment@sas.upenn.edu

simulate impact attrition during pyroclastic flows (*11*), showed a similar curve. In general, this finding allows one to invert for eroded mass from shape data alone, a result used by Szabó *et al.* (*20*), to infer the transport distance of rounded pebbles found on an alluvial fan on Mars. The ubiquity of rounding in fluvial, coastal, and aeolian environments provides qualitative evidence for similarity in particle attrition dynamics due to collisions in sediment transport. On the other hand, our discussion above makes apparent that rounding does not occur for all transport conditions but only results from chipping under a restricted subset of particle sizes and collision energies. Here, we show that bed-load transport—in particular, the collisions associated with saltation (hopping) of particles in frequent contact with the bed—selects for these requisite conditions. We present new field evidence that rounding under bed-load transport is quantitatively similar in river, coastal, and aeolian environments—except in the rare cases where rolling and sliding occur in the absence of saltation. We perform novel simulations of particle chipping by binary collisions and develop further theoretical constraints to suggest that there is a universal relation between particle circularity and attrition mass under bed load. Such universality was first proposed by Wentworth (*1*) almost 100 years ago. These results establish a robust framework for assessing the attrition rate of natural sediments using particle shape, with implications for modeling river profile evolution and understanding the origins of fine sediment.

RESULTS

Theoretical expectations for shape evolution

The guiding hypothesis of our study is that qualitative similarity in the mechanism of particle attrition leads to quantitative similarity in particle shape evolution, when cast as a function of the fraction of mass lost by attrition, $\mu = \delta m/m_0$ (*12*, *20*), where δm is the eroded mass and m_0 is the initial mass of a particle before attrition has occurred. In the context of physics and mathematics, such convergence that is independent of system details is termed "universality" (*27*). We propose that the dominant attrition mechanism for particles transported by bed-load saltation—that is, river pebbles, coastal pebbles, and aeolian sands—is chipping and that the initial conditions for particles are fragments having a common shape distribution. In this section, we lay out the rationale for anticipating generic (universal) shape evolution and define some relevant shape parameters.

We will assume that the initial shapes of particles are fragments that can be well approximated as polyhedrons (*25*), and we expect that they should evolve toward elliptical and convex shapes due to chipping (*12*). Building on the work of Firey (*28*), Bloore (*13*) proposed a geometric theory for the shape evolution of chipping particles that has since been shown to describe real pebbles reasonably well (*12*). In Bloore's model, the local (inward-normal) erosion rate (v) of a target particle depends on both the Gaussian (K) and mean (H) curvature of that particle as

$$v = 1 + 2c_1 H + c_2 K \quad (1)$$

The parameters $c_1 = \tilde{I}(4\pi)^{-1}$ and $c_2 = \tilde{A}(4\pi)^{-1}$ depend on the size of the impacting particles, where $\tilde{I}$ and $\tilde{A}$ denote the average mean curvature integral and area of the impactors, respectively [see the study of Várkonyi and Domokos (*29*) for details]. In the limit that a target particle is collided by impactors that are large, the inward erosion rate of the particle is driven only by the curvature terms and is thus diffusive in nature, driving the particle toward a sphere (*13*, *28*–*30*). This picture is consistent with the rounding of pebbles and sand grains observed in the field and laboratory studies cited above. On the other hand, if impactor particles are small, then erosion is dominated by area-driven, uniform attrition ($v \approx 1$); the target particle is predicted to evolve toward a shape with flat faces and sharp edges (*30*). The latter behavior is quite different from rounding; however, it is consistent with "sand-blasted" rock surfaces known as ventifacts and aquafacts that are sometimes found in desert and river environments, respectively (*31*, *32*).

An important consequence of bed-load transport is size-selective sorting; large particles that are rarely entrained do not move far from their source, whereas particles that are suspended move rapidly downstream and are longitudinally segregated from the bed-load population (*16*, *33*). For the case of gravel rivers where large data sets are available, it has been shown that riverbed sediments are well sorted with most particles falling within a factor of 2 of the mean grain size (*34*). Aeolian sediments are even better sorted (*35*). Thus, although bed-load sediment in rivers, coasts, and deserts is somewhat heterogeneous, to a first approximation, we can state that bed-load collisions occur among like-sized particles. Mathematically, this corresponds to the "self-dual flow" case, which holds when colliding particles are within a factor of 3 in diameter (*17*). Practically, this means that the curvature-driven terms in Eq. 1 dominate shape evolution.

Building on the work of Grayson (*36*), Domokos (*37*) showed that there is a stochastic decrease in the number of static (equilibrium) points (*38*) for particles that evolve according to Eq. 1. This property of the mathematical model appears to describe well the average shape evolution of pebbles in a natural river (*5*), where one may manually measure the number of stable (n_S) and unstable (n_U) equilibrium points—points on which a particle may rest on a horizontal surface [see the study of Domokos *et al.* (*38*) for more details]. On average, fragments have $n_S \approx n_U \approx 4.5$ (*25*), and these parameters decrease monotonically with increasing μ under chipping toward the values $n_S = n_U = 2$ for ellipsoids (*5*, *12*). The monotonicity of the evolution of equilibrium points is an inherent property of the evolution Eq. 1, and it shows a good match with the measured data (fig. S1). We regard this qualitative agreement as an independent confirmation of the applicability of Eq. 1 to natural particle attrition.

Another shape parameter one may consider is the axis ratio b/a, where b and a correspond to the intermediate and long axes [or short and long axes for a two-dimensional (2D) image] of a particle, respectively. For the case of (primarily) curvature-driven erosion, several properties of shape evolution are known from theory and experiment. Axis ratio remains approximately constant during the initial rapid rounding of a fragment until the object becomes entirely convex, and then it slowly increases with increasing μ toward $b/a = 1$ (*12*). This parameter is, however, very sensitive to fragmentation, which often occurs in the initial phase of attrition. Fragmentation preferentially breaks elongated particles (small b/a), driving them toward $b/a = 1$ (*25*) more rapidly than chipping.

The primary shape indicator we will focus on is the circularity of the particle contour, $R = 4\pi A/P^2$, where A is the area and P is the perimeter of a particle's projection in the direction of the shortest axis (*39*); $R = 1$ for a circle and $R < 1$ for any other shape. Circularity is a convenient parameter because it may be determined automatically from images, allowing large sample sizes. Moreover, one may demonstrate that circularity is not strongly affected by weak to moderate fragmentation (see the Supplementary Materials), and therefore, R may be a robust indicator of eroded mass by chipping. Little is known mathematically about roundness evolution under the 3D Bloore Eq. 1. Some properties

are known, however, for the simplified 2D case. In two dimensions, Bloore's equation reads

$$v = 1 + c\kappa \quad (2)$$

where κ is the local curvature of the eroding (target) pebble and c is the representative perimeter of impactor particles in the environment (*29*, *30*). In the limit of large impactors relative to the target particle, Eq. 2 reduces to the original shape evolution equation proposed by Firey (*28*)

$$v = c\kappa \quad (3)$$

where c is a constant. Equations 2 and 3 belong to a class of partial differential equations that have been studied for their intrinsic mathematical interest; the proof of the Poincaré conjecture (*40*) was based on curvature-driven evolution equations. In the process leading to the proof, some fascinating properties of these equations were identified, which allow us to make useful predictions about shape evolution of particles under chipping. Synthesizing existing mathematical theory (*28*, *36*, *41*, *42*) (see Methods for details), we can make several predictions about how circularity increases with mass loss due to chipping. In decreasing order of how universally they apply, we find the following properties of the $R(\mu)$ curve: (i) If the initial shapes are polygonal and we use either Eq. 2 or 3 (or even if we add frictional terms), then $R'(0) = \infty$ (where "′" refers to differentiation with respect to μ); (ii) if we use either Eq. 2 or 3, then $R'(1) = 0$; (iii) if we use Eq. 3, then $R'(\mu) > 0$; (iv) if we use Eq. 3, then $R(1) = 1$; and (v) if our initial polygons are only mildly elongated, then, numerically, we find $R''(\mu) < 0$. These predictions are summarized in Fig. 1. Considering the restricted case of curvature-driven erosion (Eq. 3) that results from collisions of particles with like-sized particles or a flat surface—relevant for well-sorted bed-load particles—these constraints may be translated into words as follows. For a polyhedron, the initial rate of rounding (at $\mu = 0$) is infinite (i) because the curvature of sharp edges is infinite, but this rate rapidly decreases with increasing μ as a particle rounds and must approach a constant when $\mu = 1$ (*36*, *42*) (ii) that is associated with a circle (iv). These conditions mean that a curve of R versus μ should be monotonically increasing (iii) and concave (sublinear) (v).

The above conditions do not allow us to analytically predict the precise form of the $R(\mu)$, which will depend on details of initial particle shape and also the relative size of the target particle to impactors. The theory does, however, place strong constraints on the shape of the $R(\mu)$ curve. Further, if the (average) initial shape and relative size of target and impactor particles are similar across different systems—as we expect they are—then a universal $R(\mu)$ is expected to arise from geometry. We empirically test this idea next, using data from a wide range of environments where chipping by bed-load saltation is expected to occur.

Empirical evidence for universal rounding of bed-load particles

Although quantitative measurements of particle shape evolution by collisions in laboratory experiments have been reported for decades, there are few data sets from natural systems (*1*, *6*, *7*). Further, direct comparison of field data requires that the same shape parameters, measured at comparable resolution, be available for all of them. We choose to first compare circularity from existing and new data sets, where we have predicted important features of the evolution of R as a function of attrition mass fraction μ. In the field, however, attrition mass is rarely known. For rivers and dune fields (with unimodal winds), it is more natural to assess particle shape as a function of distance (x) downstream from the sediment source $x = 0$.

We measured particle shape using identical image techniques (see Methods) in three different systems for which the source location and initial shape of particles could be determined (Fig. 2): a cobble-bedded river, a gypsum sand dune field, and a rotating drum experiment. River data were reported by Litwin *et al.* (*5*) and come from a 9-km profile of a steep gravel-bed channel ($b \sim 5$ cm) in northeastern Puerto Rico; the sediment source was reasonably constrained to be landslide- and weathering-derived volcaniclastic fragments in the channel headwaters, and grain shape was determined at each site as the average of 100 to 150 particles (see the study of Litwin *et al.* (*5*) for methods). The desert dune data set comes from samples collected along an 8-km transect in White Sands National Monument that was reported by Jerolmack *et al.* (*4*); sands ($b \sim 0.5$ mm) originate from a well-defined line source of angular and bladed gypsum grains, and their shape was reanalyzed here under a microscope to determine average values at each site based on ~500 particles (see Methods). The rotating drum experimental data were presented by Szabó *et al.* (*20*) and involved 80 initial limestone fragments ($b \sim 2$ cm) dropped in air repeatedly from a height of 20 cm; the shape and mass of particles were determined after N rotations,

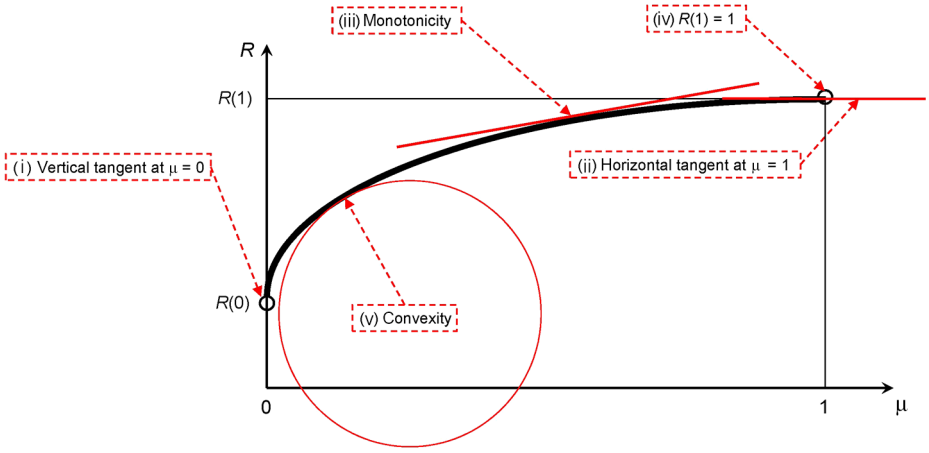

Fig. 1. Expected evolution of the roundness *R* plotted as a function of the relative mass loss μ. Properties of $R(\mu)$ in decreasing order of their universality: (i) vertical tangent at $\mu = 0$; (ii) horizontal tangent at $\mu = 1$; (iii) monotonic increase of $R(\mu)$; (iv) $R(1) = 1$; and (v) monotonic decrease of $dR/d\mu$ (convexity).

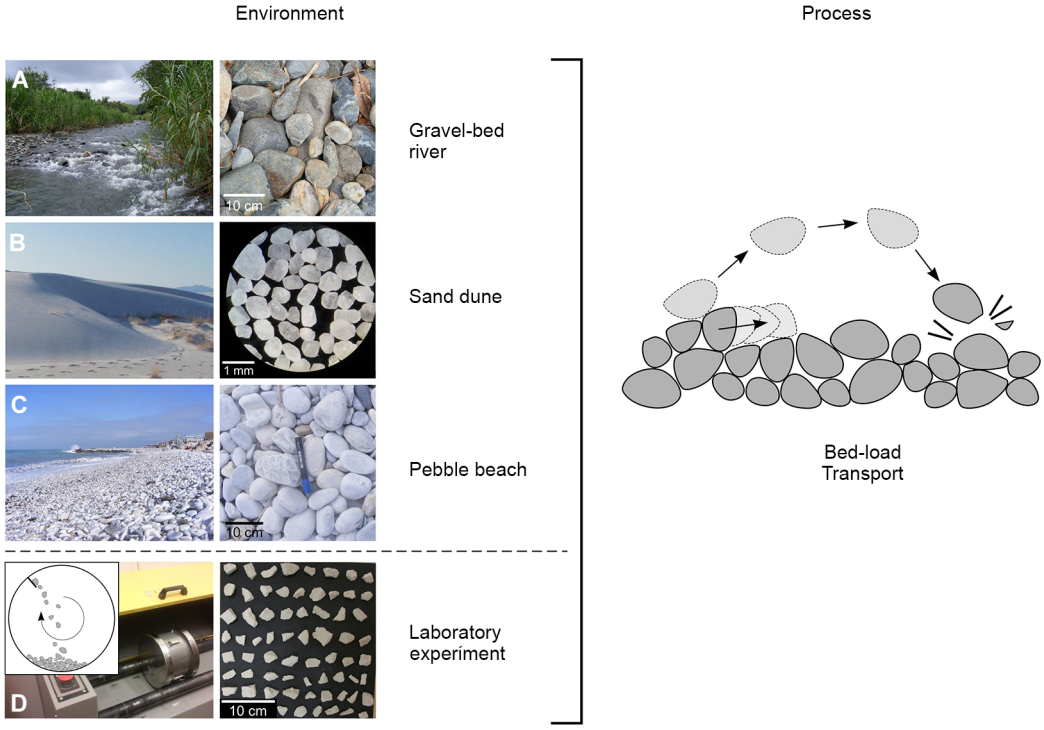

Fig. 2. Environments and sediments examined in this study. Field data were collected from different environments: (**A**) gravel-bed river in Puerto Rico, (**B**) gypsum dune field in New Mexico, (**C**) pebble beach in Marina di Pisa, and (**D**) experiment in a rotating drum. All illustrated environments select for the conditions of bed-load transport (right side) where impacts from saltation drive chipping.

which may be seen as a proxy for transport distance. The resulting circularity values for all systems are plotted as a function of transport distance, with the distance axes linearly scaled for each such that the data lie on top of each other (Fig. 3A). It must be seen as merely a coincidence that the distance axis for the river and desert data is the same scale. Notice first that the initial circularity at $x = 0$ is similar for all three systems. For the river and laboratory data, this is likely because the initial particles are fragments having a similar shape (*25*). The White Sands initial particles are crystals formed by precipitation, not fragments; it is likely coincidence that the initial circularity of these grains is comparable to those of the other systems. We see that the curves of R versus x for each system show all the qualitative features expected for R versus μ, in particular an initially rapid rounding that slows and approaches a constant rate with increasing distance. This result indicates that transport distance is linearly related to mass loss, as has been suggested in earlier studies (*5*, *11*). The former is connected to the latter by particle attrition rate; however, direct conversion between them is difficult because attrition rate depends on the velocity and frequency of bed-load collisions and also material properties (*18*). The agreement in shape evolution among these systems is encouraging, given that they involve particles of very different sizes and material strengths, transported in different fluids and collided in different ways. The addition here of aeolian sand data to the previous river and drum results (*20*) provides empirical support that rounding by chipping due to bed load is general.

We now rescale the data to test for generality in the curve of circularity as a function of attrition mass. The latter was measured for the drum experiment and inferred from a model fit to the river data [see the study of Litwin *et al.* (*5*)]. To convert x to μ for the dune field, we use the observation that saltating particles have a cylindrical shape with a constant diameter but a length that is reduced by about 20% over a distance $x \approx 4$ km (*4*). Assuming this reduction to be the result of chipping (*4*) allows us to infer $\mu \approx 0.2$ over this distance. As expected, the data from three different systems reasonably collapse onto a single curve of R against μ (Fig. 3B). We also point out that rotating drum experiments of volcanic clasts reported by Manga *et al.* (*11*) produced very similar curves of R against μ; however, we cannot quantitatively compare results because circularity depends on image resolution. To extend these results to bed-load transport by waves, we use data from a field experiment that tracked the mass and shape of radio-tagged marble pebbles ($b \sim 5$ cm) on the energetic Barbarossa Beach in Marina di Pisa, Italy (*43*). An initial batch of 240 randomly selected pebbles were tagged ($t = 0$), and recoveries were performed after $t = 3$, 8, 10, and 13 months; the average number of pebbles recovered for each survey was four, and no pebbles were recovered more than once. The results therefore consist of average shape and mass for each of the four sets of pebbles recovered at two points in time. The shapes of the pebbles at $t = 0$ varied because there was no clearly defined source location; all had experienced some degree of transport and attrition before being tagged, and therefore, we have no data for $\mu = 0$. Qualitatively, we see that initially angular pebbles experienced more rounding than initially rounded pebbles (Fig. 4). To allow comparison of the wave data to the other systems, we project the circularity of the initial pebbles associated with $t = 0$ for each set onto the curve to infer μ; it ranges from 0.13 to 0.24 (Fig. 3B). Data indicate that the change in R measured for each recovered pebble set follows the expected curve quite well. Although the starting value for μ had to be assumed, the shape evolution following additional attrition is entirely consistent with the other data (Fig. 3B and fig. S2). Together, we find strong empirical evidence that there is a unique R versus μ curve for the attrition of particles by collisions due to bed load.

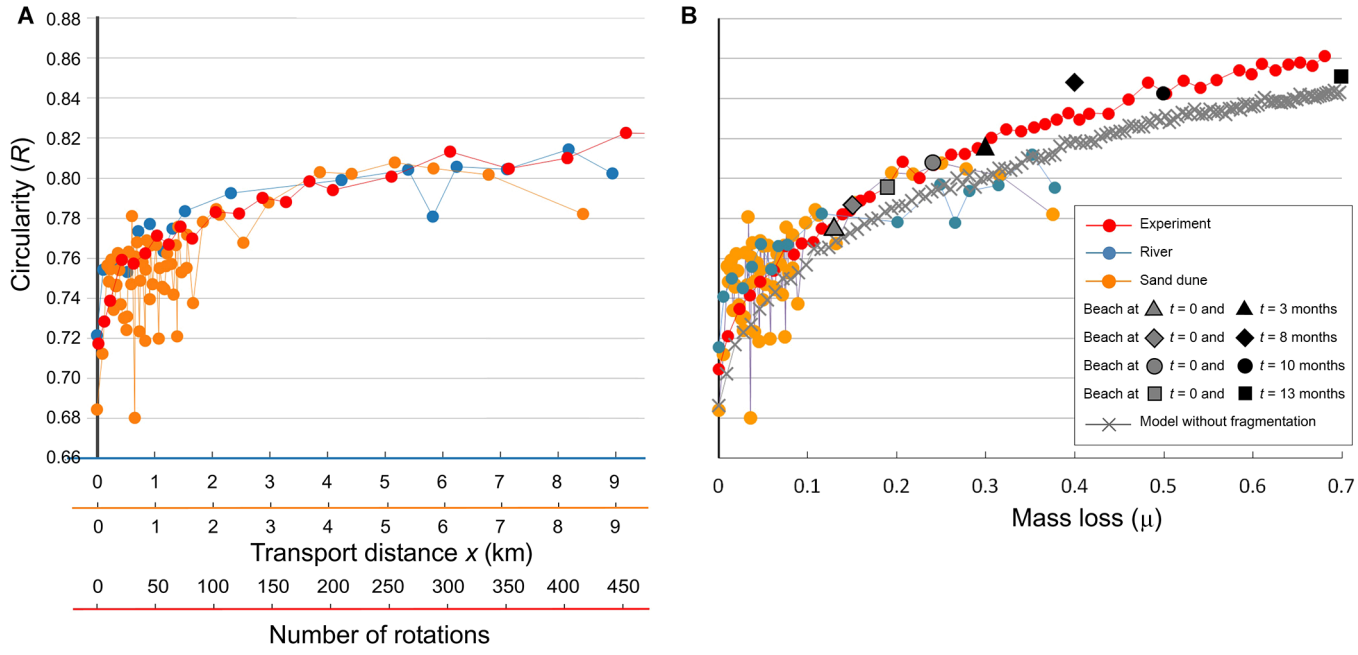

Fig. 3. Evolution of circularity. Field, experimental, and model data showing the evolution of circularity with (**A**) transport distance from source and (**B**) mass loss. Data points represent the median value of *R*. Note in (A) that axes have been linearly rescaled so that curves fall on each other; the curves of circularity naturally collapse when replotted against mass loss (B). Note that model results do not appear in (A) because transport distance is not relevant, whereas wave results are absent because initial conditions (at $x = \mu = 0$) and transport distance are not known. Initial measurements (at $t = 0$) for wave data in (B) are projected onto the curve because these particles were already partially rounded; changes in roundness following recovery of tracers, however, are consistent with other data.

Numerical chipping model for rounding

We would like to test whether the observed patterns for particle shape match predictions from a purely geometric chipping model. Solving the partial differential Eq. 1 for arbitrarily shaped particles, however, is computationally challenging. Here, we implement a stochastic, discrete event–based chipping model that has been shown to reproduce the shape evolution behavior of Eq. 1 (*12*). Moreover, the discrete model reflects more directly the way that impact chipping actually occurs. Simulation parameters are chosen to represent binary collisions among identical particles, the self-dual case (*17*), as an idealized model for bed-load transport of like-sized grains. The initial particle shape for each simulation was determined from a 3D topographic scan of an actual gypsum fragment (see Methods). In total, 21 simulation runs were carried out using a different gypsum fragment each time, and results averaged together to produce the shape evolution curves presented. At each step (collision), the simulated particle's surface is intersected with a randomly oriented plane, which removes a small, prescribed volume (chip). For a polyhedral shape, there are three possible outcomes: a vertex is removed with probability p, an edge is removed with probability q, or a face is shifted inward with probability $1 - p - q$ corresponding to inward-normal erosion ($v = 1$). Vertex and edge removal events are associated with the Gaussian and mean curvature–dependent terms in Eq. 1, respectively [see the study of Domokos *et al.* (*12*)]. For the self-dual case, the probabilities can be determined uniquely

$$p = \frac{4\pi A}{8\pi A + 2I^2} \quad \text{and} \quad q = \frac{2I^2}{8\pi A + 2I^2} \tag{4}$$

where the area A and mean curvature integral I of the particle are measured at each step, and thus, p and q are updated accordingly. Initial fragments experience 67,500 collisions over the course of a run.

The evolution of circularity with attrition mass (R versus μ) from the model matches the available data quite well (Fig. 3B). Although model results for R plot slightly below the data, this may be the result of either (i) a smaller initial value of R for the fragments used in the simulations or (ii) the presence of some fragmentation in the data (see below). It is important to emphasize that no parameters in the model were tuned to fit the data. If one needed to relax the assumption of self-duality, then parameters could be tuned to account for this. It appears that most—if not all—of the common rounding pattern of bed-load particles can be explained by chipping of initial fragments due to collisions with same-sized particles. Variables such as grain size/mass, transport medium, rock type, and collision energy will strongly influence the rate of particle attrition and may have some secondary effects on shape evolution. The origin of the generic $R(\mu)$ curve, however, appears to be geometric in nature and insensitive to these details.

Effects of fragmentation and friction

The pure chipping model reproduces the major features of the evolution of circularity in the data; however, there are aspects of shape evolution that are not captured by this simplest model. We examine this in detail for the rotating drum experiment, because this is the system for which the most information is known. The number of equilibrium points in the experiment and model follows general expectations for chipping of initial fragments; they start at a value $n_S \approx n_U \approx 4.5$ and decrease toward a value of 2 with increasing μ. However, model values are systematically offset below the experimental data (fig. S1). The mismatch is more severe for axis ratio for which model and experimental trends are qualitatively different. Values of b/a increase relatively rapidly and consistently with μ for the experiment, whereas they fluctuate and even decrease at first for the model before settling in on a pattern of slowly increasing b/a for $\mu > 0.3$ (fig. S1). The rapid increase in axis ratio for the experiment hints

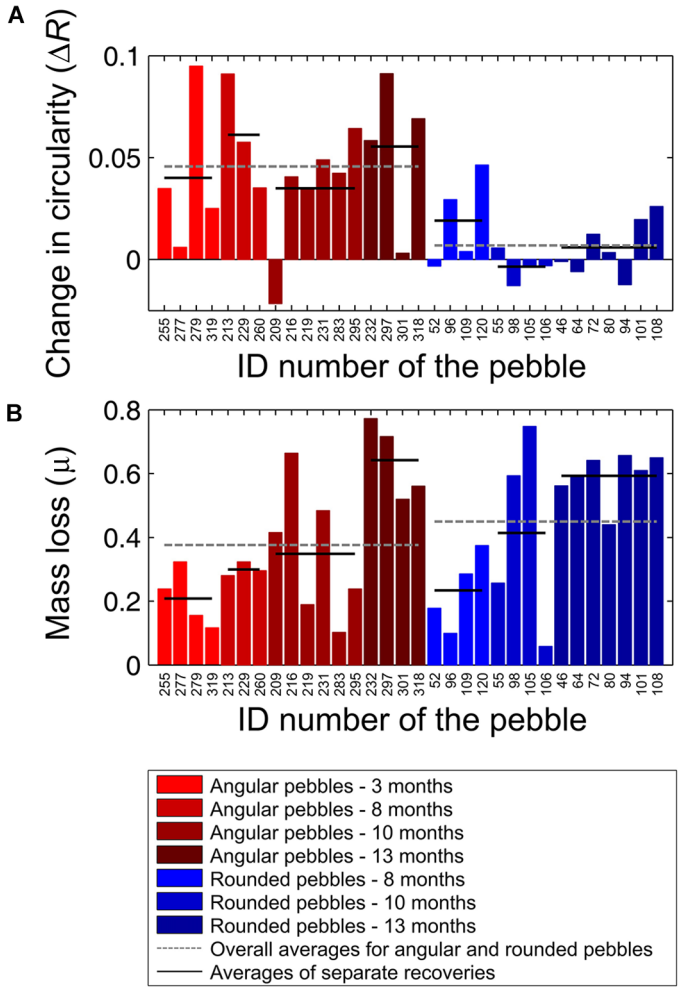

Fig. 4. Field data from Marina di Pisa of wave-transported pebbles. Red and blue show initially angular and rounded pebbles, respectively. (**A**) Change in *R* and (**B**) mass loss (μ) for the individual pebbles. The legend in (B) applies to both panels. (**C**) Examples of an initially angular (top) and initially rounded (bottom) pebble before (left) and after (right) the experiment.

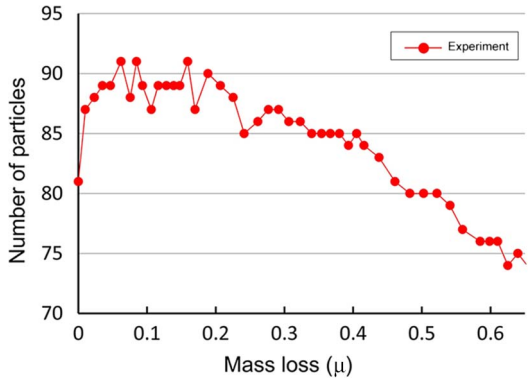

Fig. 5. Evolution of the number of particles during the rotating drum experiment on limestone fragments. The initial increase is evidence of fragmentation occurring in the beginning of the experiment.

that fragmentation may be playing a role. We observed that the number of particles in the drum first increased up to $\mu \approx 0.1$, plateaued, and then persistently decreased for $\mu > 0.2$ (Fig. 5). That pattern indicates that moderate fragmentation of the limestone particles occurred at the start of the experiment, but this effect became negligible with continuing mass loss. Trends in axis ratio and equilibrium points for the river data are similar to experiments, although, unsurprisingly, are much more erratic; fragmentation may also play a role in the initial attrition of river pebbles in the upper reaches of the profile.

To test whether fragmentation can explain deviations between model and experiment, we added a simple fragmentation component to the model that is motivated by recent simulations of Domokos *et al.* (*25*). The model is predicated on the notion that fragmentation happens preferentially to particles that are (i) elongated (low axis ratios) and (ii) at the start of their evolution. The model randomly chooses particles and times for fragmentation, and each fragmented particle is split in two with both products retained for further attrition. This is implemented probabilistically using an axis ratio–dependent parameterization of the Weibull distribution—a widely used model for predicting the time of failure (*44*)—to determine the time of fragmentation for each particle (if it happens at all). In the absence of empirical constraints, the shape parameter of the distribution was assumed to be a linear function of b/a, whereas the scale parameter was unity. The numerical chipping model with moderate fragmentation is able to reproduce empirical trends for both axis ratio and equilibrium points (Fig. 6) and even produces a modest improvement in circularity.

The data also suggest that circularity in different systems may not asymptotically approach a value of 1; rather, rounding in some systems appears to saturate at sufficiently large mass loss ratios (Fig. 6A). Recall that the saturation at the value of 1 was among the least universal features of the $R(\mu)$ curve shown in Fig. 1 and was predicted to happen only for energetic, curvature-driven abrasion. In general, the data collapse is good in the range $0 \leq \mu \leq 0.5$, whereas the agreement among disparate systems diminishes for larger values of mass loss. Previous studies have indicated that frictional abrasion becomes increasingly important in the lower-gradient portions of rivers where collision energy decreases (*5*, *45*). It has also been suggested from field observations that wave-worked pebbles initially evolve toward spherical shape but that later, in their trajectory, they become flat (*3*). Together, we suggest that bed-load attrition produces a universal rounding of rock fragments by chipping but that low-energy frictional abrasion may arise in the latter stages of pebble evolution ($\mu > 0.5$) and drive trajectories away from the universal curve.

DISCUSSION

Mechanisms and ranges for particle impact attrition

Our results show that particle shape evolves along a common curve when chipping is the dominant mode of attrition and that fragmentation and

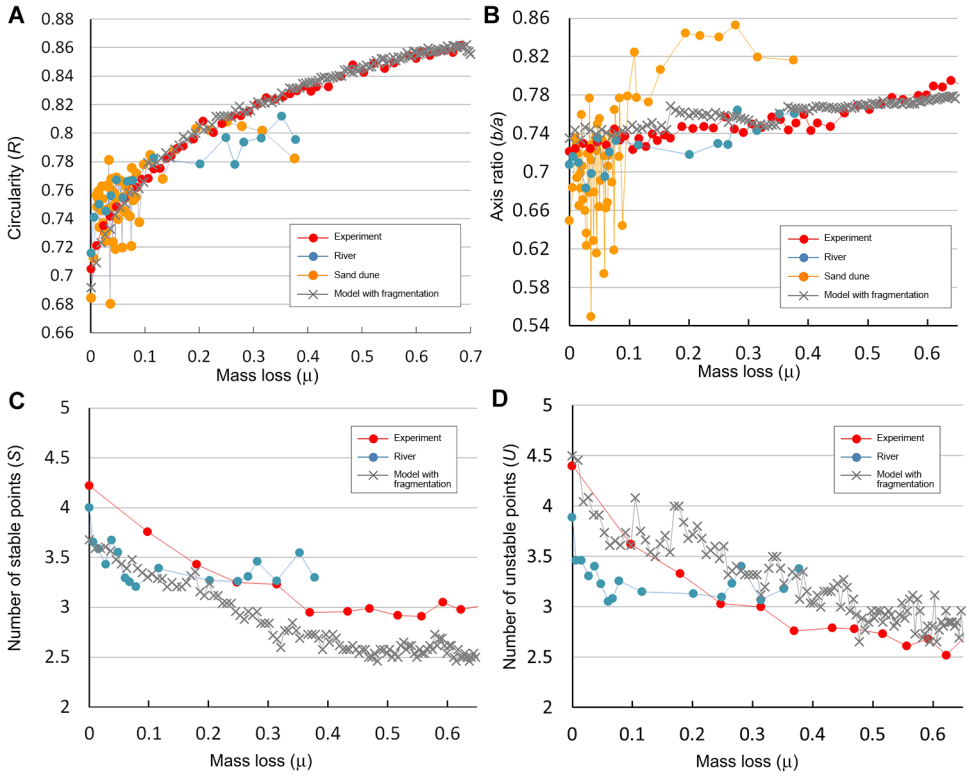

Fig. 6. Numerical chipping model with the addition of moderate fragmentation compared to available data. Shape data examined are (**A**) roundness, (**B**) axis ratio, (**C**) number of stable points, and (**D**) number of unstable points; the latter two were not available for White Sands data. Data points represent average values.

friction cause deviations from this curve. Here, we perform a scale analysis to first delineate the upper bound for chipping, that is, fragmentation, due to bed-load transport in water. The collision energy associated with particle impact is $E_i = 1/2mv_s^2$, where m is the particle mass and v_s is the velocity of a sediment grain. Bed load is a kind of dense granular flow, where it has been shown that the relevant velocity scale for collisions is the terminal fall velocity w_s (*46*). In the large-particle limit, $w_s \approx \sqrt{RgD}$ (*47*), where $R = (\rho_s - \rho_f)/\rho_f$ is the relative submerged sediment density and ρ_s, ρ_f, g, and D are sediment density, fluid density, gravity, and grain size, respectively. A characteristic value for sediment impact energy becomes $E_i \approx mRgD \sim \rho_s RgD^4$. Defining a single critical impact energy for the transition from chipping to fragmentation is an oversimplification, because even repetitive low-energy collisions may eventually lead to fragmentation by fatigue failure (*24*). Nevertheless, a useful upper bound is the one associated with the onset of intense cracking for which a single collision may produce fragmentation. This critical energy E_c, is a property of not only the material but also particle size (*48*, *49*) and shape (for example, long and thin particles fragment more easily) (*25*, *49*). The control of size is reasonably well described from data, whereas shape is less explored. The range of natural pebble shapes is limited, however, such that this influence may be secondary; one study found that the difference in critical impact energy between rounded river quartz pebbles and crushed fragments was negligible (*49*). For simplicity, we neglect shape controls here. Assuming that particles are transported underwater in saltation, we may estimate a critical particle size, D_c, associated with the onset of significant fragmentation, that is, $E_i = E_c$. Above this size, particles of a given material will always fragment under transport, whereas below this size, we expect that chipping and rounding will occur. Examining results from experimental crushing studies of quartz (ρ_s = 2650 kg/m^3) (*48*, *49*), we find for particles in the size range 10^{-3} m < D < 10^{-1} m that the data may be reasonably described by the relation $E_c = 0.2m/D \sim \rho_s D^2$, where m has units of kilograms and E_c has units of Joules. Using this relation and setting $E_i = E_c$, we estimate that $D_c \sim 10^{-1}$ m, meaning that fragmentation of common quartz pebbles should become dominant for grains of order decimeter and larger if they are transported. Large, immobile boulders in streams will resist fragmentation because they are not transported. Limestone particles had comparable but reduced impact energies—around half the value of quartz—over the same range and so should have moderately smaller values for D_c. These results are consistent with laboratory experiments (*10*, *20*, *26*) and observations from rivers (*5*, *50*). Impact energy for aeolian transport of sand grains is well below the critical value so fragmentation is negligible, although weak dust aggregates have been proposed to experience breakup by fragmentation (*51*).

Bed-load transport causes frequent collisions among particles due to saltation. The results above allow us to demonstrate that these collisions are in the range where chipping should dominate attrition, in water and air. Consider a river with a bed of cobbles that is at the border between fragmentation and chipping, that is, D = 0.1 m. It has been found empirically that the dimensionless fluid stress (τ_*) of gravel-bed rivers depends on river slope (S), $\tau_* = 2.18S + 0.021$ (*52*). It has also been observed that fragmentation of river rocks becomes significant in steep, mountain headwaters (*10*, *50*). Assuming normal flow conditions $\tau_* = hS/(RD)$, where h is the flow depth and R = 1.65 for quartz grains in water, and that shallow mountainous streams have flow depths comparable to grain size so that $D/h \sim 10^0$, the slope of the river associated with the onset of fragmentation would be expected to be of order $S \sim 10^{-1}$. This slope corresponds to the observed transition in sediment transport

mode from bed load to debris flows (*53*) in rivers. Results suggest that highly energetic debris flows produce fractured rocks, whereas the transition to bed load is associated with a transition to chipping and rounding of these rock fragments.

We propose that the lower boundary of chipping, and the transition to frictional abrasion, may be cast in terms of the minimum energy required for a particle to transition from rolling to saltation, E_s. Bed-load particles underwater move not only by saltation but also by rolling and sliding, which should contribute to frictional abrasion rather than chipping. Rolling and sliding are negligible for aeolian bed-load transport, where entrainment by impact collision is always dominant (*35*). We posit that the large difference in attrition rates between frictional abrasion and chipping leads to a dominance of the latter, unless saltation is negligible. For the range of fluid stresses associated with bed-load transport in rivers, some saltation is likely always present; pure rolling and sliding only occur in the immediate vicinity of the threshold of motion (*54*). Considering a particle sitting on a bed of like-sized grains, we can cast the threshold for saltation in terms of the energy required to lift a particle from its pocket, $E_s \approx (\rho_s - \rho_f)gVD/2 \sim (\rho_s - \rho_f)gD^4$, where V the is particle volume. For particles with kinetic energy smaller than this value, they should move by rolling and sliding but not saltation. Although some authors have attributed flat beach pebbles to initial fragment conditions and/or sorting (*1*–*3*)—and we concur that initial conditions can play an important role—it was recognized early on that some wave-worked pebbles may move primarily by rolling and sliding. The presence of disk-shaped pebbles on the landward margins of beaches (*3*) suggests that these may be environments in which saltation is minimal, and where we hypothesize that transport occurs very close to the threshold of motion. As pointed out by Landon (*2*): "The flat pebble, traveling by 'skidding,' is worn mostly on its flat surfaces…Wave action would eventually produce flat pebbles on any beach from any originally shaped forms." This idea was codified into a geometric model for frictional abrasion by Domokos and Gibbons (*17*), which predicts shape evolution by sliding/rolling that is consistent with observations. Considering field data from rivers and beaches, it appears that initial rounding of fragments is dominated by chipping (saltation) but that late-stage shape evolution of pebbles as they move into lower-energy environments is influenced by frictional abrasion (rolling/sliding) (*2*, *5*, *45*). We expect a narrow range in phase space, associated with transport right at the threshold of motion, where the shape evolution of underwater pebbles will be dominated by frictional abrasion—a condition found on some beaches and in some portions of rivers.

Conditions for universality

We propose a phase diagram that distills the ideas here to delineate the ranges of the three forms of attrition—frictional abrasion, chipping, and fragmentation—and also expected shape evolution as a function of the ratio (impactor particle size)/(target particle size) (x axis), particle energy (z axis), and particle size (y axis) (Fig. 7). To illustrate the relevant ranges, consider the example of a representative quartz pebble, with diameter $D = 2$ cm. There are two relevant characteristic energy scales in the phase diagram: (i) The critical energy associated with fragmentation E_c is the upper bound for chipping and is a property of the pebble material and size (and potentially shape), and (ii) the energy associated with the onset of saltation E_s is the boundary between chipping and frictional abrasion and is a property of pebble size or mass. Our example pebble $E_c = 0.2m/D \sim 10^0$ J and $E_s \approx (\rho_s - \rho_f)gVD/2 \sim 10^{-3}$ J, and therefore, the phase space for chipping is large (Fig. 7). However, there is a critical particle size, D_c, related to the critical energy E_c (through settling velocity), associated with grains large enough that they will always fragment if they are subject to collision. For very large or very weak pebbles, the saltation energy/size becomes comparable to the critical value, and hence, the phase space for chipping can be eliminated. As shown above, this is the case for quartz particles of order $D \sim 10$ cm and larger (in water). Although qualitative and somewhat speculative at this point, the phase diagram serves to place the chipping and rounding results developed above in the context of the full range of attrition processes, as well as to guide future research toward assessing the boundaries among these processes.

The considerations above place three constraints on the attrition of particles by bed-load transport: (i) it is dominated by collisions among similarly-sized particles; (ii) the dominant mechanism is chipping, therefore shape evolution can be described by Bloore's Eq. 1 (except in special cases at beaches); and (iii) initial particles are likely fragments produced by a different mechanism. This region of phase space associated with bed load, where we expect geometric

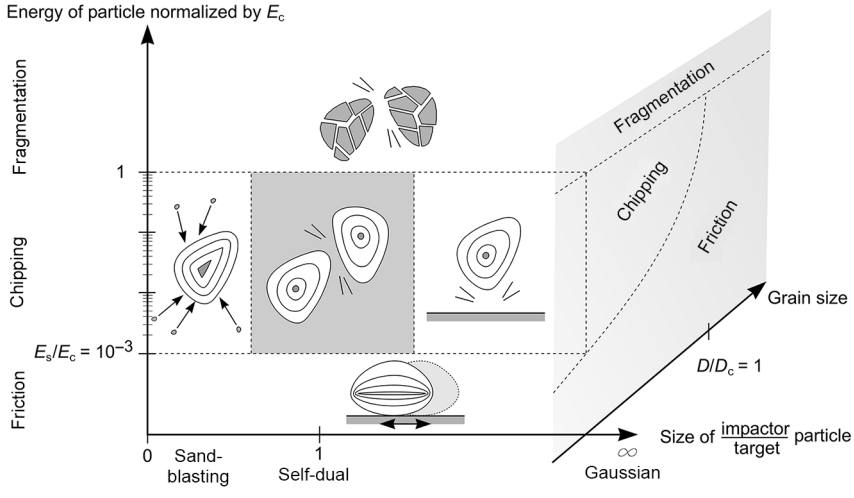

Fig. 7. Phase space for attrition: Effect of relative size, normalized collision energy, and normalized grain size on attrition mode. The zone corresponding to chipping and self-dual collisions is highlighted in gray; this is the region associated with bed-load transport.

rounding, is highlighted in Fig. 7 and corresponds to the "self-dual" and "chipping" regions.

Summary and implications

In principle, the shape evolution of particles undergoing attrition is sensitive to the ratio of impactor to target particle size, the initial shape, and the energy of collisions. However, nature selects for a subset of conditions that lead to a universal rounding behavior. Pebbles in rivers and coasts, sand grains in a desert dune field, and limestone rocks in a drum all exhibit a remarkably consistent trend in the evolution of circularity when cast as function of attrition mass. What these different systems have in common is that particle attrition occurs because of low-energy collisions. The ability of an idealized numerical model to reproduce the $R(\mu)$ curve demonstrates that this generic behavior is a consequence of three constraints: (i) similar initial shapes, (ii) self-dual collisions, and (iii) attrition by chipping. The fragmentation by physical and chemical weathering of parent rocks (*25*) produces fragments having a universal size-shape relationship, which serve as the initial material for bed-load transport. Size-selective sorting of particles by bed load ensures that collisions are typically among like-sized particles. Finally, the energy of collisions associated with the bed-load transport in air and water is small enough (relative to rock strength) that fragmentation is typically rare, but large enough to overcome viscous damping and to dominate over frictional abrasion, leading to chipping. These findings may also extend to attrition in pyroclastic flows, where rounding consistent with chipping has been observed (*11*). We note here that although our findings derive from a study of interparticle collisions, they have implications for erosion of bedrock by particles that should be further explored. A microscopic examination of rock surfaces eroded by aeolian sandblasting showed clear evidence for chipping (*31*), and fluvial bedrock surfaces eroded by cobbles were observed to exhibit a similar appearance (*32*).

This study shows that the quantification of particle shape, and its evolution through transport time/distance, may be used to infer the significance of fragmentation, chipping, and frictional abrasion mechanisms. Circularity is sensitive to chipping and insensitive to moderate fragmentation (see Methods and the Supplementary Materials) and shows a similar evolution under attrition for all bed-load systems examined here. We propose that deviations from this universal curve (Fig. 1) indicate transport regimes where chipping is not the dominant mode of attrition—for example, in the latter stages of pebble rounding, where frictional abrasion may be important. Axis ratio, on the other hand, is sensitive to fragmentation but changes only slowly because of chipping. Rapid increases in axis ratio through transport time/distance can result from even modest fragmentation and, in principle, could be used to infer a fragmentation rate—although this would require more theoretical development. An advantage of both circularity and axis ratio is that they may be determined from images and therefore can be applied to particles ranging from sand and smaller up to immobile boulders. One disadvantage is that these parameters are 2D and therefore may be insensitive to some aspects of mass loss. The number of equilibrium points represents a 3D metric that is moderately sensitive to both chipping and fragmentation, providing complementary information to the other shape parameters. Recent work has demonstrated that equilibrium points are powerful and mathematically convenient parameters for classifying pebble shapes (*38*) and documenting their evolution under attrition (*5*, *45*). Measurements of equilibria, however, are currently limited to particles that may be manipulated by hand (*38*). Future theoretical and technological progress may allow determination of chipping and fragmentation rates based on equilibria. Turning to natural systems, gravity-driven flows in hillslopes and steep rivers, such as rock falls, landslides, debris flows, and pyroclastic flows, are highly energetic and result in fragmentation of rocks (*11*, *26*). We would expect to see rapid reductions in axis ratio in these settings, but little change in circularity and equilibria, under particle attrition. Downstream decreases in grain size and slope, however, lead to a transition in rivers to bed-load transport and an associated change in the particle attrition mechanism to chipping accompanied by rounding. This is consistent with observed changes in the rate and style of particle breakdown from "unsound pebbles" in river headwaters (fragmentation) to "sound pebbles" downstream (chipping) (*50*), a pattern that is also observed through time in our drum experiments. Pebbles transported by waves are typically highly rounded and thus in the "sound" category where chipping dominates, although large pebbles may occasionally fragment. We posit that flat pebbles often found at the margins of beaches have experienced frictional abrasion due to rolling and sliding in the absence of significant collision—and hence transport that is just at the threshold of motion. Aeolian sands almost certainly erode in the pure chipping regime.

Ever since Sternberg proposed in 1875 the empirical "law" that particle size decreases exponentially with downstream distance in a river (*55*), researchers have debated the relative contributions of size-selective transport and attrition to this trend (*6*, *8*, *10*, *16*, *24*, *33*, *56*). Sorting and attrition both can cause an exponential decline in grain size (*5*). Laboratory experiments are useful for assessing rates of chipping attrition under bed load; however, researchers have raised questions about whether and how these results can be scaled up to the field (*8*, *10*, *56*). Shape provides a means to settle these debates, by using the $R(\mu)$ curve to directly estimate particle attrition rate in landscapes; however, this approach is not without its caveats. In the simplest case of a localized point source of initial fragments—for example, landslide-derived sediments delivered over a limited length in the headwaters of a river—we expect that the ensemble-averaged value for roundness (measured from many particles) is $R(0) \approx 0.7$ at $x = 0$. If one can safely assume that particles downstream of this source region are transported as bed load, then ensemble-averaged values for R can be determined from images alone moving downstream along a river profile and inverted directly for the attrition mass fraction μ (Fig. 7). One may then use Sternberg's law rewritten in terms of attrition mass fraction (*20*), $1 - \mu = e^{-k_e x}$, to determine the diminution coefficient k_e associated with attrition by chipping. If source particles are more spatially distributed (rather than a point source) and heterogeneous in shape (not fresh fragments), then a location suitably downstream of the source region may be chosen and characterized as the initial conditions. This average roundness may then be projected onto the $R(\mu)$ curve, and downstream changes in roundness may be differenced to determine mass loss and the diminution coefficient. In the most challenging situation where rock fragments are delivered continuously along the length of the river simultaneously with rounding (*57*), downstream trends of ensemble-averaged roundness will not be useful for determining attrition rate. Here, the only recourse is to examine downstream rounding of known tracers rather than the entire pebble population. Tagged particles could be recovered periodically, as was done for our beach experiments; however, attrition may be negligible over reasonable study periods (years) if transport is infrequent. Alternatively, one could isolate downstream shape change of pebbles having a distinct lithology that is known to originate from a spatially localized source.

Determinations of attrition rate from roundness will be most accurate for $R < 0.85$, where rounding is most rapid and frictional abrasion

appears to be negligible. We note, however, that care must be taken because R is highly resolution-dependent (see Methods). For the Mameyes River pebbles in Puerto Rico, it was estimated that $k_e \approx 0.05\ km^{-1}$ (*5*) and that chipping attrition accounts for around 40% of the total decrease in pebble mass over a 10-km distance. The value determined here for the gypsum sand of the White Sands dune field is (coincidentally) similar, implying a similar contribution of attrition to overall fining. Estimates for quartz-sand deserts have not been made but are likely much lower than gypsum. Shape data indicate that the wave-driven pebbles of Barbarossa Beach in Italy follow the same evolution as the river and dune systems; however, the diminution coefficient cannot be directly estimated because the transport distance of particles is not unidirectional. Surveyed positions of pebbles indicate that their mean-squared displacement (MSD) grows approximately linearly with time, consistent with Brownian motion (fig. S4). Using the framework of 2D random walks (see the Supplementary Materials), and assuming that pebbles move in discrete hops that are on the order of a particle diameter (*58*), we can estimate the transport distance $d \sim MSD/b$. By plotting measured mass loss against estimated transport distance, the data permit an exponential fit and the estimation of the diminution coefficient (fig. S4). The value determined for these tracer pebbles, $k_e \approx 0.01\ km^{-1}$, is the same as the common value for river pebbles made of hard rocks and supports the idea that collision energetics are comparable in these systems. However, the diminution coefficient may be an order of magnitude larger for softer limestone pebbles (*10*, *20*).

Finally, chipping attrition from bed load produces fine sediment; impact indentation produces "platelets" having a volume significantly smaller than the parent particle (*14*). Collisions of fluvial pebbles produce sand and smaller grains that help build floodplains and beaches (*16*), aeolian sands produce silt and dust that contribute to loess accumulations and cloud nuclei (*51*, *59*), and pyroclastic flows grind angular volcanic rocks to produce ash (*11*). The ability to determine mass loss from particle shape provides a means to estimate the fine-sediment production rate associated with bed-load transport. Future research should examine the size and shape distributions of the daughter products of chipping, for a range of parent materials and sizes. Quantifying the role of physical weathering in sediment production will allow researchers to improve models for landscape evolution over geologic time (*57*) and the emission of dust that contributes to climate change (*51*, *59*).

METHODS

Evolution of circularity

It is relatively easy to see that if the initial shape at zero mass loss $\mu = 0$ is a convex polygon, then the evolution under Eq. 2 results in a vertical tangent for the $R(\mu)$ curve at $\mu = 0$. Here, we give a nonrigorous, although intuitive, 2D argument, which could be turned into a rigorous proof. It is known for the $v = c\kappa$, that is, purely curvature-driven evolution (*36*), that for the length L of the perimeter, we have $dL/dt = -\int \kappa^2 ds$. In any arbitrary small, fixed interval containing a corner, the previous integral will be arbitrarily large at $\mu = 0$, predicting that the perimeter of the curve will shrink (initially) at infinite speed. Because the area shrinks only at finite speed, the circularity R will increase at infinite speed at $\mu = 0$. The constant inward-normal term in Eq. 2 will certainly not change this fact because it reduces both the area and the perimeter at finite speed. In the case of the $v = c\kappa$ evolution, it follows from the main theorem by Gage and Hamilton (*42*) that at $\mu = 1$ (when the particle vanishes), the $R(\mu)$ curve will have a horizontal tangent. Here again, the constant term in Eq. 2 does not influence the horizontal tangent; as for vanishingly small particles, the curvature term will dominate the evolution. Combined with Gage's result on the monotonicity (*41*), in case of convex polygonal initial shapes, we expect the $R(\mu)$ curve to start with a vertical tangent, grow monotonically, and end with a horizontal tangent where the particle vanishes. Numerical experiments show that the convexity of the curve will mainly depend on the number of vertices and the axis ratio b/a of the initial polygonal shape. For rectangles, we found the critical axis ratio [above which the $R(\mu)$ function is concave] to be $b/a = 0.377$, and for rhombical shapes to be $b/a = 0.189$, and these numbers appear to be the upper and lower bounds for the critical values of polygons with four vertices. Natural fragments tend to be polyhedral, with polygonal planar projections with four to six vertices and moderate elongations $b/a > 0.4$ (*25*). So, we can conclude that the expected, "typical" $R(\mu)$ trajectory for curvature-driven attrition processes starting from natural fragments will be qualitatively similar to the curve shown in Fig. 1.

Data collection and image analysis

Details on the sampling locations and protocol for the gravel-bed river in Puerto Rico can be found in the study of Litwin *et al.* (*5*); a total of 100 to 150 pebbles were collected and imaged at each of the 17 sites, and mass loss was estimated using the method reported by Szabó *et al.* (*20*). Sampling locations and methods for White Sands dunes can be found in the study of Jerolmack *et al.* (*4*). Sand samples from 57 sites of the transect were imaged under a microscope, arranging the grains so that they did not touch each other. Only grains with $b > 250\ \mu m$ were analyzed because this is the size range expected to travel in saltation, not in suspension where attrition is negligible (*4*). Sample size was between 252 and 1226 for each site, with a mean value of 545. The wave data involved the selection at random of 90- to 150-mm-diameter (a axis) marble pebbles on Barbarossa Beach in Marina di Pisa that were then equipped with a 30-mm-diameter transponder. The pebbles were prepared using the same method as reported by Bertoni *et al.* (*60*) for a former experiment on the same beach; these papers also describe the morphology of the beach, the radio-frequency identifier (RFID) technology, and the experimental protocols. Details on the laboratory experiment can be found in the study of Szabó *et al.* (*20*): A total of 80 limestone fragments were collided in a rotating drum equipped with a paddle (Fig. 2D). Fragments were imaged and their weight was recorded after a certain number of rotations.

For the pebbles from Puerto Rico, Marina di Pisa, and the rotating drum, Adobe Photoshop's Quick Selection Tool was applied to trace the grain contours as described in the study of Szabó *et al.* (*20*). Contours of sand grains from White Sands were extracted using the thresholding tool in ImageJ. Measuring R on image contours must be done carefully because the value of R depends on the resolution of the image (*20*). Therefore, all images were resized to approximately have the same resolution, 200 pixels per grain contour, with the method described in the study of Szabó *et al.* (*20*).

SUPPLEMENTARY MATERIALS

Supplementary material for this article is available at http://advances.sciencemag.org/cgi/content/full/4/3/eaao4946/DC1

Model results without fragmentation

Evolution of equilibrium points for the wave data

Effect of fragmentation on axis ratio and circularity

Estimating transport distance for the beach data

fig. S1. Numerical chipping model without fragmentation compared to available data.

fig. S2. Field data from Marina di Pisa showing change in the number of equilibrium points.

fig. S3. β, γ, and β/γ.

fig. S4. Transport and mass loss of wave-driven pebbles at Marina di Pisa.

REFERENCES AND NOTES

1. C. K. Wentworth, A laboratory and field study of cobble abrasion. *J. Geol.* **27**, 507–521, (1919).
2. R. E. Landon, An analysis of beach pebble abrasion and transportation. *J. Geol.* **38**, 437–446, (1930).
3. B. J. Bluck, Sedimentation of beach gravels; examples from South Wales. *J. Sediment. Res.* **37**, 128–156, (1967).
4. D. J. Jerolmack, M. D. Reitz, R. L. Martin, Sorting out abrasion in a gypsum dune field. *J. Geophys. Res. Earth* **116**, F02003 (2011).
5. M. K. Litwin, T. Szabó, D. J. Jerolmack, G. Domokos, Quantifying the significance of abrasion and selective transport for downstream fluvial grain size evolution. *J. Geophys. Res. Earth Surf.* **119**, 2412–2429 (2014).
6. W. C. Krumbein, The effects of abrasion on the size, shape and roundness of rock fragments. *J. Geol.* **49**, 482–520 (1941).
7. Ph. H. Kuenen, Experimental abrasion of pebbles: 2. Rolling by current. *J. Geol.* **64**, 336–368 (1956).
8. Y. Kodama. Experimental study of abrasion and its role in producing downstream fining in gravel-bed rivers. *J. Sediment. Res.* **64**, 76–85 (1994).
9. D. J. Durian, H. Bideaud, P. Duringer, A. Schröder, F. Thalmann, C. M. Marques, What is in a pebble shape? *Phys. Rev. Lett.* **97**, 028001 (2006).
10. M. Attal, J. Lavé, Pebble abrasion during fluvial transport: Experimental results and implications for the evolution of the sediment load along rivers. *J. Geophys. Res.* **114**, F04023 (2009).
11. M. Manga, A. Patel, J. Dufek, Rounding of pumice clasts during transport: Field measurements and laboratory studies. *Bull. Volcanol.* **73**, 321–333, (2011).
12. G. Domokos, D. J. Jerolmack, A. Á. Sipos, Á. Török, How river rocks round: Resolving the shape-size paradox. *PLOS ONE* **9**, e88657 (2014).
13. F. J. Bloore, The shape of pebbles. *J. Int. Assoc. Math. Geol.* **9**, 113–122, 1977.
14. M. Ghadiri, Z. Zhang, Impact attrition of particulate solids. Part 1: A theoretical model of chipping. *Chem. Eng. Sci.* **57**, 3659–3669 (2002).
15. P. H. Kuenen, Experimental abrasion; 3, fluviatile action on sand. *Am. J. Sci.* **257**, 172–190 (1959).
16. D. J. Jerolmack, T. A. Brzinski III, Equivalence of abrupt grain-size transitions in alluvial rivers and eolian sand seas: A hypothesis. *Geology* **38**, 719–722 (2010).
17. G. Domokos, G. W. Gibbons, The evolution of pebble size and shape in space and time. *Proc. R. Soc. Lond. A* **468**, 3059–3079 2012.
18. L. S. Sklar, W. E. Dietrich, A mechanistic model for river incision into bedrock by saltating bed load. *Water Resour. Res.* **40**, W06301 (2004).
19. K. L. Miller, M. D. Reitz, D. J. Jerolmack, Generalized sorting profile of alluvial fans. *Geophys. Res. Lett.* **41**, 7191–7199 (2014).
20. T. Szabó, G. Domokos, J. P. Grotzinger, D. J. Jerolmack, Reconstructing the transport history of pebbles on Mars. *Nat. Commun.* **6**, 8366 (2015).
21. E. Perfect, Fractal models for the fragmentation of rocks and soils: A review. *Eng. Geol.* **48**, 185–198 (1997).
22. F. Kun, H. J. Herrmann, Transition from damage to fragmentation in collision of solids. *Phys. Rev. E* **59**, 2623 (1999).
23. D. E. Grady, Length scales and size distributions in dynamic fragmentation. *Int. J. Fract.* **163**, 85–99 (2010).
24. A. J. Moss, P. H. Walker, J. Hutka, Fragmentation of granitic quartz in water. *Sedimentology* **20**, 489–511 (1973).
25. G. Domokos, F. Kun, A. Á. Sipos, T. Szabó, Universality of fragment shapes. *Sci. Rep.* **5**, 9147 (2015).
26. O. Arabnia, L. S. Sklar, Experimental study of particle size reduction in geophysical granular flows. *Int. J. Eros. Control Eng.* **9**, 122–129 (2016).
27. A.-L. Barabási, H. E. Stanley, *Fractal Concepts in Surface Growth* (Cambridge Univ. Press, 1995).
28. W. J. Firey. Shapes of worn stones. *Mathematika* **21**, 1–11 (1974).
29. P. L. Várkonyi, G. Domokos, A general model for collision-based abrasion processes. *IMA J. Appl. Math.* **76**, 47–56 (2011).
30. G. Domokos, A. Á. Sipos, P.L. Várkonyi, Countinuous and discrete models for abrasion processes. *Period. Polytech. Archit.* **40**, 3–8 (2009).
31. J. E. Laity, N. T. Bridges, Ventifacts on Earth and Mars: Analytical, field, and laboratory studies supporting sand abrasion and windward feature development. *Geomorphology* **105**, 202–217 (2009).
32. A. Wilson, N. Hovius, J. M. Turowski, Upstream-facing convex surfaces: Bedrock bedforms produced by fluvial bedload abrasion. *Geomorphology* **180**, 187–204 (2013).
33. R. Ferguson, T. Hoey, S. Wathen, A. Werritty, Field evidence for rapid downstream fining of river gravels through selective transport. *Geology* **24**, 179–182 (1996).
34. J. J. Fedele, C. Paola, Similarity solutions for fluvial sediment fining by selective deposition. *J. Geophys. Res. Earth* **112**, F02038 (2007).
35. R. A. Bagnold, *The Physics of Wind Blown Sand and Desert Dunes* (Methuen & Company, 1941).
36. M. A. Grayson, The heat equation shrinks embedded plane curves to round points. *J. Differ. Geom.* **26**, 285–314 (1987).
37. G. Domokos, Monotonicity of spatial critical points evolving under curvature-driven flows. *J. Nonlinear. Sci.* **25**, 247–275 (2015).
38. G. Domokos, A. Sipos, T. Szabó, P. Várkonyi, Pebbles, shapes, and equilibria. *Math. Geosci.* **42**, 29–47 (2010).
39. S. J. Blott, K. Pye, Particle shape: A review and new methods of characterization and classification. *Sedimentology* **55**, 31–63 (2008).
40. G. Perelman, Ricci flow with surgery on three-manifolds (ArXiv preprint, 2003); https://arxiv.org/abs/math/0303109.
41. M. E. Gage, An isoperimetric inequality with applications to curve shortening. *Duke Math. J.* **50**, 1225–1229 (1983).
42. M. Gage, R. S. Hamilton, The heat equation shrinking convex plane curves. *J. Differ. Geom.* **23**, 69–96 (1986).
43. D. Bertoni, G. Sarti, E. Grottoli, P. Ciavola, A. Pozzebon, G. Domokos, T. Novák-Szabó, Impressive abrasion rates of marked pebbles on a coarse-clastic beach within a 13-month timespan. *Mar. Geol.* **381**, 175–180 (2016).
44. H. Rinne, *The Weibull Distribution: A Handbook* (CRC Press, 2008).
45. T. Szabó, S. Fityus, G. Domokos, Abrasion model of downstream changes in grain shape and size along the Williams River, Australia. *J. Geophys. Res. Earth Surf.* **118**, 2059–2071 (2013).
46. M. Houssais, C. P. Ortiz, D. J. Durian, D. J. Jerolmack, Onset of sediment transport is a continuous transition driven by fluid shear and granular creep. *Nat. Commun.* **6**, 6527 (2015).
47. R. I. Ferguson, M. Church, A simple universal equation for grain settling velocity. *J. Sediment. Res.* **74**, 933–937 (2004).
48. S. Yashima, Y. Kanda, S. Sano, Relationships between particle size and fracture energy or impact velocity required to fracture as estimated from single particle crushing. *Powder Technol.* **51**, 277–282 (1987).
49. L. M. Tavares, R. P. King, Single-particle fracture under impact loading. *Int. J. Miner. Process.* **54**, 1–28 (1998).
50. J. Adams, Wear of unsound pebbles in river headwaters. *Science* **203**, 171–172 (1979).
51. J. F. Kok, A scaling theory for the size distribution of emitted dust aerosols suggests climate models underestimate the size of the global dust cycle. *Proc. Natl. Acad. Sci. U.S.A.* **108**, 1016–1021 (2011).
52. E. R. Mueller, J. Pitlick, J. M. Nelson, Variation in the reference shields stress for bed load transport in gravel-bed streams and rivers. *Water Resour. Res.* **41**, W04006 (2005).
53. J. Stock, W. E. Dietrich, Valley incision by debris flows: Evidence of a topographic signature. *Water Resour. Res.* **39**, 1089 (2003).
54. J. E. Abbott, J. R. D. Francis, Saltation and suspension trajectories of solid grains in a water stream. *Philos. Trans. A Math. Phys. Eng. Sci.* **284**, 225–254 (1977).
55. H. Sternberg, *Untersuchungen Über Längen-und Querprofil GeschiebefÜhrender Flüsse* (Zeitschrift für Bauwesen, 1875).
56. J. Lewin, P. A. Brewer, Laboratory simulation of clast abrasion. *Earth Surf. Process. Landf.* **27**, 145–164 (2002).
57. L. S. Sklar, W. E. Dietrich, The role of sediment in controlling steady-state bedrock channel slope: Implications of the saltation–abrasion incision model. *Geomorphology* **82**, 58–83 (2006).
58. E. Lajeunesse, L. Malverti, F. Charru, Bed load transport in turbulent flow at the grain scale: Experiments and modeling. *J. Geophys. Res. Earth* **115**, F04001 (2010).
59. O. Crouvi, R. Amit, Y. Enzel, A. R. Gillespie, Active sand seas and the formation of desert loess. *Quat. Sci. Rev.* **29**, 2087–2098 (2010).
60. D. Bertoni, G. Sarti, G. Benelli, A. Pozzebon, In situ abrasion of marked pebbles on two coarse-clastic beaches (Marina di Pisa, Italy). *Ital. J. Geosci.* **131**, 205–214 (2012).

Acknowledgments: We thank M. Grayson for the discussions on the evolution of circularity. **Funding:** Research was supported by the Korányi Fellowship to T.N.-S.; Hungarian OTKA grant 119245 to G.D., A.Á.S., and T.N.-S.; and the NSF Luquillo Critical Zone Observatory grant EAR-1331841 to D.J.J. **Author contributions:** T.N.-S. performed the data analysis; A.Á.S. developed the numerical model; S.S. performed the image analysis on the sand grains from White Sands; D.B., A.P., E.G., G.S., and P.C. performed the RFID experiment in Marina di Pisa; G.D. developed the theoretical part of the paper; and D.J.J. supervised the research. D.J.J., T.N.-S., G.D., and A.Á.S. wrote the paper. **Competing interests:** The authors declare that they have no competing interests. **Data availability:** All data needed to evaluate the conclusions in the paper are present in the paper and/or the Supplementary Materials. Additional data related to this paper may be requested from the authors.

Submitted 2 August 2017
Accepted 12 February 2018
Published 28 March 2018
10.1126/sciadv.aao4946

Citation: T. Novák-Szabó, A. Á. Sipos, S. Shaw, D. Bertoni, A. Pozzebon, E. Grottoli, G. Sarti, P. Ciavola, G. Domokos, D. J. Jerolmack, Universal characteristics of particle shape evolution by bed-load chipping. *Sci. Adv.* **4**, eaao4946 (2018).

Science Advances

Universal characteristics of particle shape evolution by bed-load chipping

Tímea Novák-Szabó, András Árpád Sipos, Sam Shaw, Duccio Bertoni, Alessandro Pozzebon, Edoardo Grottoli, Giovanni Sarti, Paolo Ciavola, Gábor Domokos and Douglas J. Jerolmack

Sci Adv **4** (3), eaao4946.
DOI: 10.1126/sciadv.aao4946